Damage assessment of wind sand erosion on composite car body based on computational fluid dynamics

Lijun Li [1, a, *], Yongli Jin [2, b]

[1]School of Transportation Science and Engineering, Beihang University, Beijing 100191, China

[2]713th Research Institute of China Shipbuilding Industry Corporation, Zhengzhou 450015, China

[a]lljstc@126.com, [b]julianking@sina.com

Abstract. With the requirements of weight reduction on vehicles, carbon fiber reinforced plastic (CFRP) will be utilized extensively in car bodies. Wind sand erosion can damage the surface of solid greatly, and it is different from an ordinary fatigue damage. Hence, it is necessary to study the factors and methods to assess damage of wind sand erosion on CFRP car body. In this work, the material properties of CFRP are measured through experimental methods. A FE model is established in software Workbench to simulate the wind sand erosion on CFRP car body. With the model, we can determine sand erosion rate to predict the erosion of car body surfaces over time. It is found that the sand erosion rate increases significantly with the wind velocity and the sand erosion rate is nearly proportional to the diameter of sand. This paper provides a theoretical guide for the design of CFRP car body under wind sand impact loads.

Keywords: Sand erosion, CFRP, Car body, Damage assessment, CFD.

1. Introduction

Composite car body is transferring from the laboratory to the factory with superior material properties. Carbon fiber reinforced plastics (CFRPs) have been developed extensively as an excellent composite. Wind sand erosion is different from an ordinary fatigue damage. Investigations into wind sand erosion on the surfaces of CFRP body are important for durability and reliability of vehicles used in the sandstorm areas (e.g., Middle East, Middle Asia).

To date, a number of experimental and computational researches regarding sand erosion have been conducted. Erosion caused by the solid particles received more disciplined study after approximately 1960 [1]. G.P. Tilly and Wendy Sage [2] have studied the failure mechanism of sand erosion by high speed photography and inspection of the surface topography of steel, nylon 66, and fibers under impact loads. Impact process of sand particles onto metal surface includes a complex reciprocal effect between the solid particles and the contact surface [3]. Yang Shichao et al. [4] have considered the influences of different conditions in wind sand erosion on mechanical properties of a glass fiber/unsaturated polyester composite material. The results show the change of sand impact angle is a weak factor, and wind velocity and exposure time are strong factors. However erosion rate of structure surface has not drawn attention. Wong, Chong Y., et al. [5] have proposed a method to computationally simulate the material damage of a flat aluminum plate with the central hole caused by sand erosion. It is shown that the erosion loss can be predicted accurately using computational fluid dynamics (CFD) model.

Hence, wind sand erosion of CFRP car body can be predicted using CFD model. The erosion rate of surface should be established. In this paper, the external airflow field model of a commercially available car is established in software Workbench. With the aerodynamic characteristics of car body (e.g., coefficient of drag) which are known, the model can be modified and verified to get good accuracy. With the model, the factors and methods to assess damage of wind sand erosion on CFRP car body are studied. The purpose of this paper is to provide a theoretical guide for the design of CFRP car body under wind sand impact loads.

2. Numerical simulation and verification of airflow field for car body

The numerical simulation model of car body is established in CFD software Workbench, and the external airflow field is established simultaneously. To facilitate calculating, the car body model has been simplified without rearview mirrors, etc. Since the model has axial symmetry, the paper builds half model. Basic dimensions of model as follows length 4,500 mm, width (symmetrically taking a half) 1,000 mm, height 1,400 mm derived from one car listing. The computational domain is set as 15,000 mm long, 5,000 mm wide and 7,000 mm high. The model adopts tetrahedron meshing. Fig. 1 shows details of the finite element model geometry and mesh.

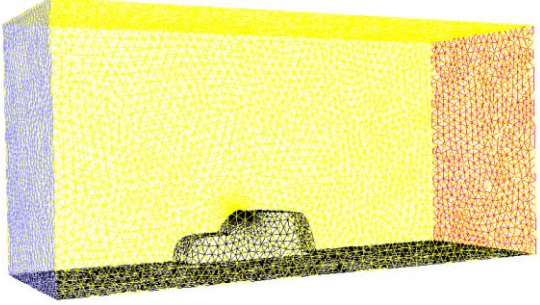

Fig. 1 Overall FE model of car body

Fig. 2 shows the pressure variations of computational domain including car body surface at 30 m/s velocity. The wind flow characteristics of car body is well simulated.

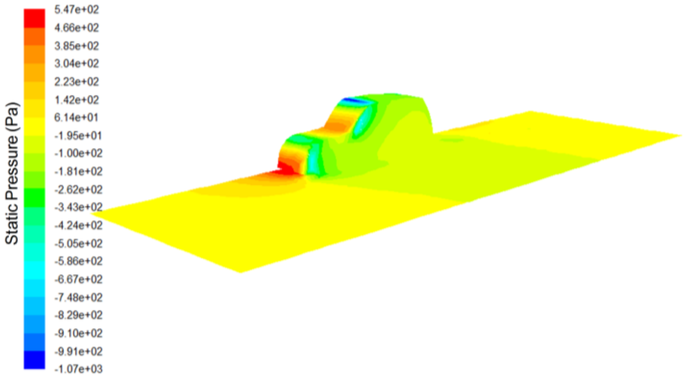

Fig. 2 Pressure contour under 30m/s impact velocity

Coefficient of drag (Cd) has a large influence over the aerodynamic performance of the car. We have simulated three inlet velocity conditions, 20 m/s, 30 m/s and 40 m/s, to obtain the aerodynamic characteristics of the car body. The results are listed in Tab.1.

Table.1 The comparison of Cd under different impact velocities

Velocity (m/s)	Wind resistance (N)	Forward projection area (m2)	Cd	Reference Cd
20	214.41344	2.057798	0.425	0.42
30	478.45452	2.057798	0.422	0.42
40	844.99626	2.057798	0.419	0.42

From Tab.1, we find that simulation Cd is close to reference Cd. The FE model of car body and external airflow field have good accuracy. Therefore, the model can be applied to wind sand erosion simulation.

3. Damage assessment of wind sand erosion on car body

In order to obtain the material properties of CFRP in the simulation, we made the specimens for testing. The epoxy matrix is E51, and the fiber is T700-12K carbon fiber. Fiber volume fraction is 65% and the thickness of each lamina is 0.175 mm. The CFRP plate is a layup of eight layers [6]. American Society of Testing Materials (ASTM) D3039/D3039M-08 is adopted as the test standard in this work. The 90 ° specimens are shown in Fig. 3, and the 0 ° specimens are similar except that the effective length (Ls) is 250 mm.

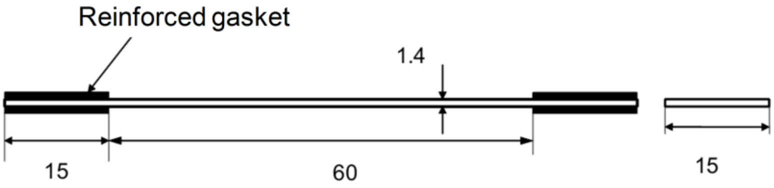

(a) Schematic diagram of tensile specimens [6]

(b) Photograph of tensile specimens

Fig. 3 Diagram of tensile specimens

The experiment equipment is shown in Fig. 4. The quasi-static tensile tests were conducted at velocity of 2 mm/min, and the displacement was controlled by extensometer. The tensile force was measured by sensors.

Fig. 4 Test device for material properties measurement

According to the results from tests, two curves of specimen in both directions are shown in Fig. 5.

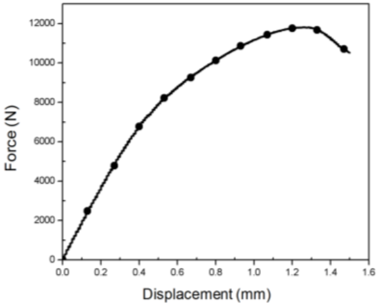

(a) 0 °specimens

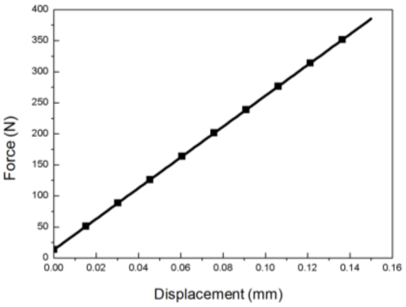

(b) 90 °specimens

Fig. 5 Curves of force versus displacement for CFRP plates under tensile loads

The material properties of CFRP are given in Tab.2. In the table, 0 ° ply fiber direction tensile modulus (E_x) 133.2 GPA and 90 ° ply fiber direction tensile modulus (E_y) 8.42 GPA are obtained by calculating test data shown in Fig. 5. Other parameters are provided by the CFRP manufacturer.

Tab.2 Mechanical properties of CFRP at ambient temperature [6]

E_x (Gpa)	E_y (Gpa)	G_{xy} (Gpa)	ν_{xy}	ν_{yz}	X_t (Mpa)
133.2	8.42	4.62	0.33	0.48	1590
X_c (Mpa)	Y_c (Mpa)	Y_t (Mpa)	S_{xy} (Mpa)	S_{xz} (Mpa)	S_{yz} (Mpa)
1250	192	49	98.2	98.2	98.2

For the wind sand erosion on car body made by CFRP materials simulation, we produce the model coupled with a CFD solver to predict erosion rate. In the model, sand is set as discrete phase and wind is set as continuous phase. The CFD model adopts standard second-order K-ε equations. In the simulation, we have studied wind velocity and sand diameter influences on sand erosion rate. According to wind scale list, we select three typical velocity as research subjects which are 10 m/s (five-stage wind), 20 m/s (eight-stage wind) and 30 m/s (eleven-stage wind). Furthermore, three typical size of sand (0.1 mm, 0.15 mm and 0.2 mm) are studied. Fig. 6 shows the tracks of sand particles with the time when wind velocity is 20 m/s and sand diameter is 0.15 mm, and inlet logo demonstrates the injection direction of wind and sand.

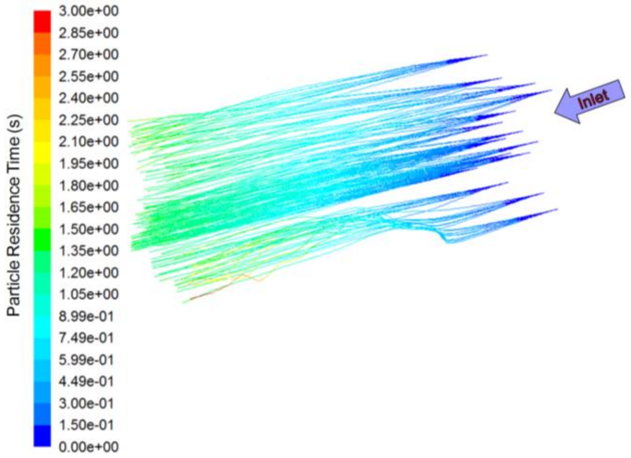

Fig. 6 Moving tracks of the discrete sand particles (at 20 m/s speed, with 0.15 mm sand diameter)

Fig. 7 shows the sand erosion rate distribution on car body after sand impacts. From the contour, the sand erosion is heterogeneous, and the front edge of car roof is impacted more seriously.

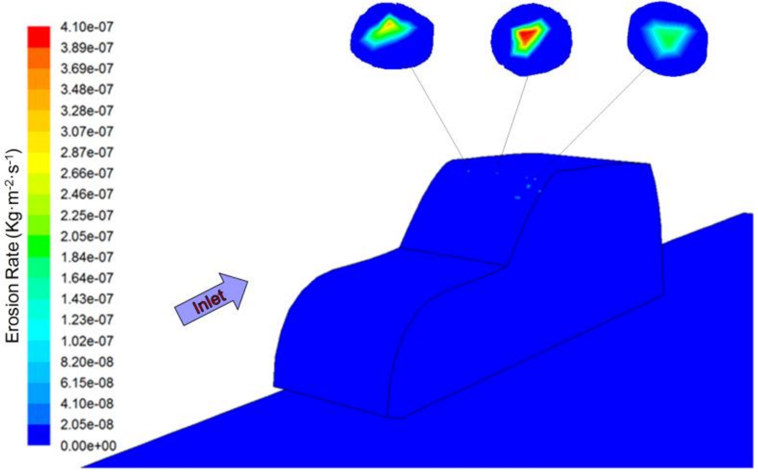

Fig. 7 Contour of wind sand erosion rate (at 20 m/s speed, with 0.15 mm sand diameter)

Because the failure of car body is determined by the earliest failure part, we choose the maximum erosion rate as the damage assessment index of CFRP car body under wind sand erosion load. The results are drawn in Fig. 9 and Fig. 10.

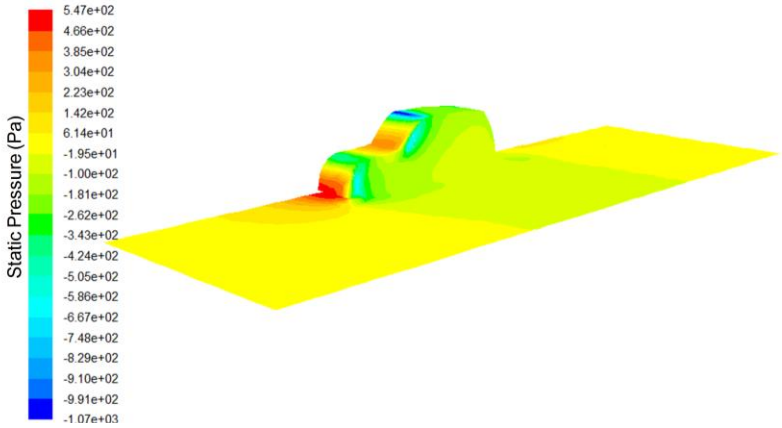

Fig. 8 Contour of pressure (at 20 m/s speed, with 0.15 mm sand diameter)

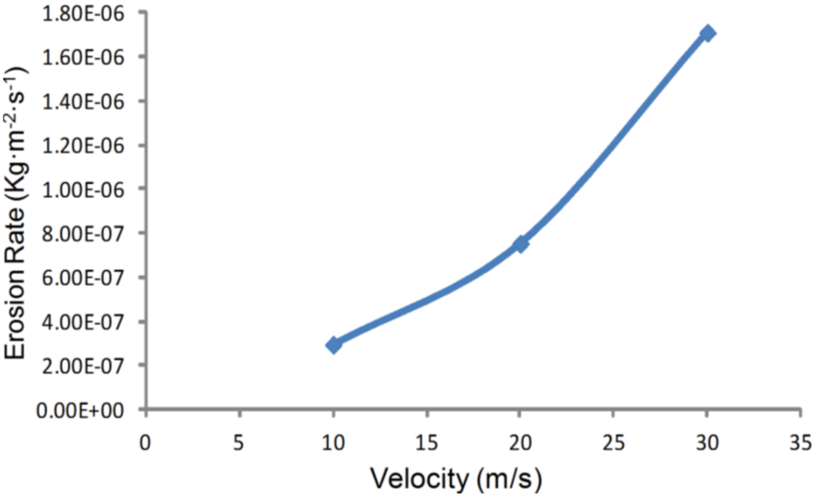

Fig. 9 Curve of sand erosion rate versus wind velocity

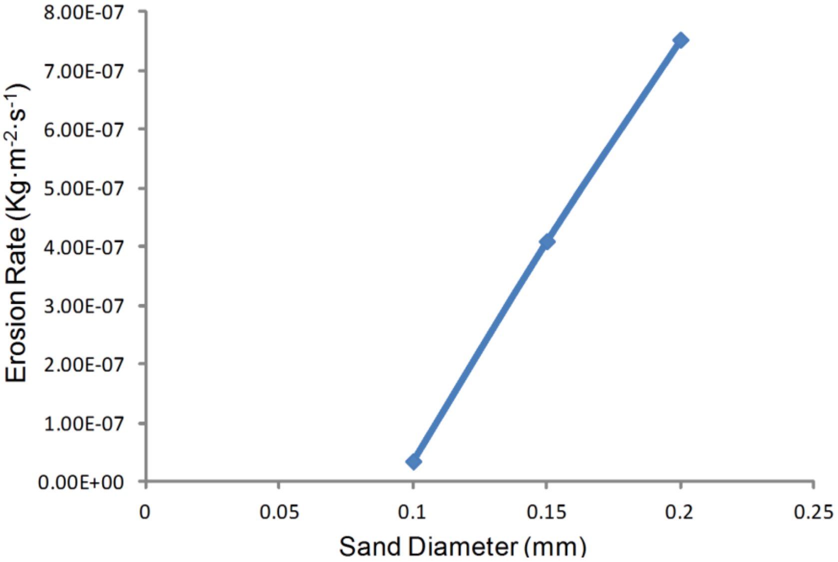

Fig. 10 Curve of sand erosion rate versus sand diameter

From the curve in Fig. 9, the sand erosion rate increases significantly with the wind velocity. Because the higher velocity of wind improves the kinetic energy of sand impacts on car body, the damage of car body surface is aggravated. Hence, the wind velocity has a great influence on sand erosion. From the curve in Fig. 10, we can observe that the sand erosion rate is nearly proportional to the diameter of sand. While the diameter of sand becomes larger, the quality would increase correspondingly. So the kinetic energy would be improved during the wind sand impacting on car body. Finally, the erosion rate increases and the damage is aggravated.

4. Conclusions

In this paper, the material properties of CFRP panels applied in car bodies are measured through experimental methods. The FE model of a CFRP car body is established in software Workbench to study the wind sand erosion effect. An effective method of damage assessment of wind sand erosion on car body is provided. From the simulation results, we can find that the sand erosion rate increases significantly with the wind velocity and the sand erosion rate is nearly proportional to the diameter of sand. Hence, for those CFRP car body applied in desert region, the wind sand erosion must be considered in the durability design. The simulation method can help us predict the damage of CFRP car body quantitatively under wind sand erosion loads.

References

[1] G. P. Tilly, Sand erosion of metals and plastics: a brief review, Wear, vol. 14 (1969), 241-248.

[2] G. P. Tilly, and Wendy Sage, The interaction of particle and material behaviour in erosion processes, Wear, vol. 16 (1970), 447-465.

[3] P.V. Rao, D.H. Buckley, Solid impingement erosion mechanisms and characterization of erosion resistance of ductile metals, NASA Technical Memorandum, 1982, 50-62.

[4] Yang, Shichao, et al, Anti-wind-and-sand erosion properties of GF/unsaturated polyester composite, Acta Materiae Compositae Sinica, vol. 28 (2011), 77-82. (In Chinese)

[5] Wong, Chong Y., et al, Predicting the material loss around a hole due to sand erosion, Wear, vol. 276 (2012), 1-15.

[6] Juanjuan Sun, Lingyu Sun, Junmin Du, Taikun Wang: Impact damage and residual strength of composite joints in car bodies, ASME 2013 International Mechanical Engineering Congress and Exposition (San Diego, CA, USA, November 15-21, 2013), 13: V013T14A030.